

Coefficient-Free Blood Pressure Estimation Based on Pulse Transit Time–Cuff Pressure Dependence

Mohamad Forouzanfar*, *Student Member, IEEE*, Saif Ahmad, Izmail Batkin, Hilmi R. Dajani, *Senior Member, IEEE*, Voicu Z. Groza, *Fellow, IEEE*, and Miodrag Bolic, *Senior Member, IEEE*

Abstract—Oscillometry is a popular technique for automatic estimation of blood pressure (BP). However, most of the oscillometric algorithms rely on empirical coefficients for systolic and diastolic pressure evaluation that may differ in various patient populations, rendering the technique unreliable. A promising complementary technique for automatic estimation of BP, based on the dependence of pulse transit time (PTT) on cuff pressure (CP) (PTT–CP mapping), has been proposed in the literature. However, a theoretical grounding for this technique and a nonparametric BP estimation approach are still missing. In this paper, we propose a novel coefficient-free BP estimation method based on PTT–CP dependence. PTT is mathematically modeled as a function of arterial lumen area under the cuff. It is then analytically shown that PTT–CP mappings computed from various points on the arterial pulses can be used to directly estimate systolic, diastolic, and mean arterial pressure without empirical coefficients. Analytical results are cross-validated with a pilot investigation on ten healthy subjects where 150 simultaneous electrocardiogram and oscillometric BP recordings are analyzed. The results are encouraging whereby the mean absolute errors of the proposed method in estimating systolic and diastolic pressures are 5.31 and 4.51 mmHg, respectively, relative to the Food and Drug Administration approved Omron monitor. Our work thus shows promise toward providing robust and objective BP estimation in a variety of patients and monitoring situations.

Index Terms—Blood pressure (BP), estimation, mathematical model, oscillometry, pulse transit time (PTT).

I. INTRODUCTION

AUTOMATIC noninvasive blood pressure (BP) measurement and monitoring is an important clinical tool [1]. It is now common for medical practitioners to manage drug

therapies/treatment regimens for regulating BP using noninvasive BP evaluation [2]. Accuracy in BP measurement is of paramount importance for effective treatment and patient management. It has been shown that a BP estimation error of as little as 5% can lead to a 25% increased risk of morbid consequences such as myocardial infarction and stroke [3].

Most automatic noninvasive BP devices employ the oscillometric method [4]. Briefly, cuff pressure (CP) is reduced gradually from a level above systolic blood pressure (SBP) to a level below diastolic blood pressure (DBP), during which the monitor records arterial pulsations sensed by the cuff. The CP at which arterial pulsations attain maximum amplitude is considered the mean arterial pressure (MAP). Empirical coefficients are then used on the CP–pulse amplitude mapping, most often specific to the device, to estimate SBP and DBP.

Several challenges exist for the automatic oscillometric BP estimation method. First, since it is solely based on changes in arterial pulse amplitudes, it fails to provide accurate estimation in several conditions such as atrial fibrillation, obesity, and atherosclerosis, whereby pulse amplitudes may be weak/erratic [5]–[9]. More significantly, the method relies on empirical coefficients to estimate SBP and DBP, rendering it somewhat unreliable in diverse patient populations and measurement scenarios [10], [11].

Previous studies have tried to overcome the aforementioned problems by employing an alternative time-based method for automatic BP estimation [12]–[15]. These studies investigated the dependence of pulse transit time (PTT), the time delay between electrocardiogram (ECG) R-peaks and arterial pulses, on CP, for BP estimation. However, these techniques were not suitably developed; for example, they required pressure/ECG sensors auxiliary to the cuff. Problems like these defeated the simplicity and straightforwardness of the oscillometric BP estimation method. In a recent article, our research group proposed an ergonomic integration of the PTT–CP method with the oscillometric method for accurate BP measurement [16]. The results were promising whereby our method achieved grade A as per British Hypertension Society (BHS). However, our work still relied on using empirical coefficients on the PTT–CP mapping for SBP and DBP estimation. Moreover, the focus of that work was on the validation of the method/algorithms that we had developed and not on developing a theoretical foundation of the analysis. To the best of our knowledge, no previous work (including ours—[16]) provided a theoretical explanation of the PTT–CP method along with employing a nonparametric (coefficient-free) method for SBP/DBP estimation from either the PTT–CP dependence or oscillometry.

Manuscript received September 22, 2012; revised December 5, 2012 and January 18, 2013; accepted January 20, 2013. Date of publication January 28, 2013; date of current version June 24, 2013. This work was supported in part by the Natural Sciences and Engineering Research Council of Canada, the Ontario Centres of Excellence, the Ontario Ministry of Economic Development and Innovation, and the Ontario Ministry of Training, Colleges and Universities. Asterisk indicates corresponding author.

*M. Forouzanfar is with the School of Electrical Engineering and Computer Science, University of Ottawa, Ottawa, ON K1N 6N5, Canada (e-mail: mforo040@eecs.uottawa.ca).

S. Ahmad, H. R. Dajani, V. Z. Groza, and M. Bolic are with the School of Electrical Engineering and Computer Science, University of Ottawa, Ottawa, ON K1N 6N5, Canada (e-mail: sahmad@eecs.uottawa.ca; hdajani@eecs.uottawa.ca; groza@eecs.uottawa.ca; mbolic@eecs.uottawa.ca).

I. Batkin is with the School of Electrical Engineering and Computer Science, University of Ottawa, Ottawa, ON K1N 6N5, Canada, and also with Ottawa General Hospital, Ottawa, ON K1H 8LC, Canada (e-mail: vbatkin@rogers.com).

Digital Object Identifier 10.1109/TBME.2013.2243148

In this paper, we 1) develop a theoretical framework for the PTT–CP BP estimation method, which is an extension of previous modeling work done on oscillometry alone [10], [17]–[21]; 2) show that with the developed model, SBP, DBP, and MAP can be determined directly from maxima of PTT–CP mappings without empirical coefficients when PTT is measured from ECG R-peak to the oscillometric pulse peak, trough, and zero-crossing, respectively; and 3) cross-validate the theoretical findings of 2) by estimating BP from 150 actual ECG and oscillometric recordings obtained from ten healthy subjects using our prototype [16] and comparing it with analogous BP estimates made by Food and Drug Administration (FDA)-approved Omron monitor (HEM-790IT). Our proposed method is accurately able to estimate BP values using the developed theoretical model. With the empirical data, our method achieves a mean absolute error (MAE) of 5.31 mmHg for SBP, 4.51 mmHg for DBP, and 5.74 mmHg for MAP, relative to the Omron device.

This paper is organized as follows. In Section II, theory of BP estimation based on PTT–CP dependence is developed. In Section III, our theoretical findings are cross-validated by analyzing actual oscillometric BP and ECG recordings. The conclusion is presented in Section IV, and the limitations of the study and the future work are provided in Section V.

II. METHODOLOGY

In this section, a mathematical model of oscillometry is derived to describe the interaction between the cuff and the artery. This model is then utilized to build a model for the PTT based on which the coefficient-free estimation of BP is proposed.

A. Oscillometry Model

When the cuff is not placed on the arm, the arterial pressure is the only pressure that is exerted on the arterial wall. The arterial pressure varies over each heartbeat from a minimum called diastolic pressure to a maximum called systolic pressure. The arithmetic mean of the arterial pressure signal samples during each heartbeat is called MAP. Since the arterial pressure is always greater than zero, the brachial artery in this situation is always stretched and distended. When the oscillometric cuff is placed around the arm, the arterial wall confronts another pressure in the opposite direction of the arterial pressure. To study the arterial vessel behavior in this condition, the transmural pressure p_t , defined as the difference in pressure between the two sides of the arterial wall, should be considered [10]:

$$p_t(t) = p_a(t) - p_c(t) \quad (1)$$

where t is the time index, $p_a(t)$ represents the arterial pressure, and $p_c(t)$ is the CP.

In oscillometry, the cuff is inflated to a suprasystolic pressure (SSP) and then slowly released to a subdiastolic pressure (SDP). Assuming that the deflation is performed linearly over time, the CP can be modeled as follows:

$$p_c(t) = SSP - rt \quad (2)$$

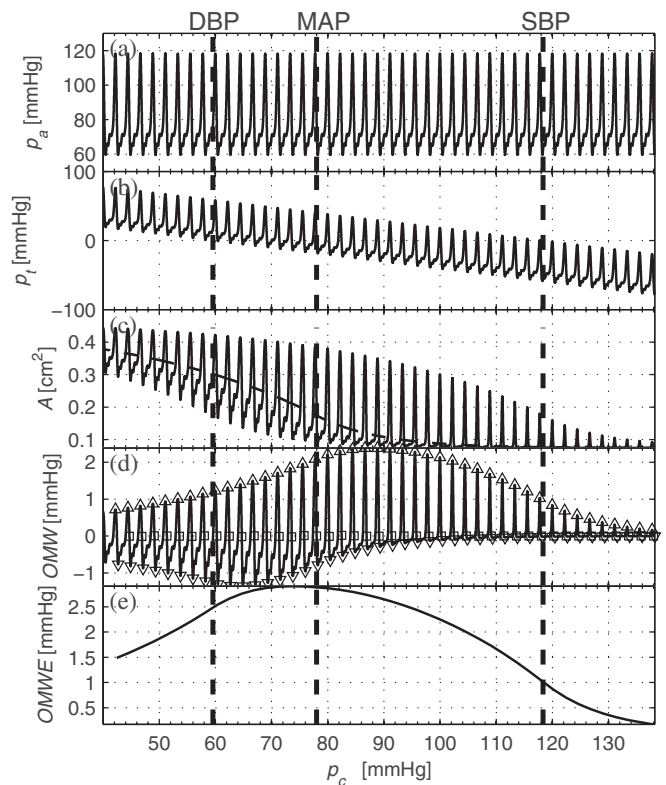


Fig. 1. Oscillometry model. (a) Simulated arterial pressure. (b) Simulated transmural pressure. (c) Simulated ALA. (d) Simulated OMW using equation (8). The peaks, troughs, and zeros are shown with upward triangles, downward triangles, and squares, respectively. (e) OMWE. The vertical dashed lines from left to right show the points at which CP is equal to DBP, MAP, and SBP, respectively.

where r is the deflation rate which is kept constant between 1 to 4 mmHg/s [16]. It should be noted that if the deflation deviates from linearity, the CP model can be readily adjusted and, as will be seen later, the model of CP will not affect our proposed coefficient-free BP estimation method.

The arterial pressure is modeled as a sum of N harmonically related sinusoids with a dc component equal to MAP [10]:

$$p_a(t) = \text{MAP} + \sum_{i=1}^N \alpha_i \cos(2\pi f_c i t + \phi_i) \quad (3)$$

where f_c is the average cardiac rate, and α_i and ϕ_i represent the average amplitude and phase of the i th harmonic of the cardiac signal over the deflation period. A more complete model of the arterial pressure waveform including the respiration effect and arterial pressure parameters variation can be found in [22]. Studying the effects of respiration and time variation of the arterial pressure parameters on PTT is not the focus of this paper and will be addressed in future work.

Fig. 1(a) shows a simulated arterial pressure waveform. The parameters of the arterial pressure model were found by fitting (3) to a real arterial pressure waveform taken from the MIMIC II database [23]. Four harmonics were considered to be adequate as they carry most of the signal power. The extracted parameter values are MAP = 78.32 mmHg, $f_c = 81$ beats/min, $\alpha_1 = 18.36$ mmHg, $\alpha_2 = 13.38$ mmHg, $\alpha_3 =$

7.00 mmHg, $\alpha_4 = 3.14$ mmHg, $\phi_1 = 1.18$ rad, $\phi_2 = 1.32$ rad, $\phi_3 = 1.34$ rad, and $\phi_4 = -4.39$ rad. The SBP and DBP values for this signal are 118.31 and 59.56 mmHg, respectively. Fig. 1(b) illustrates the simulated transmural pressure. Both arterial and transmural pressures are plotted as a function of the CP. The cuff is linearly deflated from an SSP (here 140 mmHg) to an SDP (here 40 mmHg) using a deflation rate of 3 mmHg/s. The time sampling period T_s was set to 1 ms. It should be noted that the selected arterial pressure parameters are only used for the purpose of illustration. We will show in Section II-B that our proposed BP estimation method is independent of the arterial pressure parameters.

The study of the arterial mechanics at different transmural pressures is of critical importance in modeling oscillometry [17]. There have been several research studies on modeling the arterial pressure–area relationship [10], [18]–[21]. It has been found that when the transmural pressure is positive, the arterial wall is stretched and distended and the arterial lumen area (ALA) exhibits a circular shape. In contrast, with negative transmural pressures, the arterial wall is bent and collapsed. During collapse, the ALA changes its shape from circular to elliptical until it becomes flat and occluded. The most common model for the arterial pressure–area relationship is the exponential model proposed in [24] and [25] and adopted in many research studies on oscillometry [19], [21], [26]–[29], defined as follows:

$$A(t) = \begin{cases} A_0 e^{ap_t(t)}, & \text{for } p_t(t) \leq 0 \\ A_{\max} + (A_0 - A_{\max})e^{-bp_t(t)}, & \text{for } p_t(t) \geq 0 \end{cases} \quad (4)$$

where $A(t)$ represents the ALA, a and b are compliance indices that are an indication of the arterial stiffness, A_0 represents the ALA at zero transmural pressure, and A_{\max} is the fully expanded ALA. All the model parameters a , b , A_0 , and A_{\max} are always positive. In order to obtain a differentiable ALA function in all its domain including $p_t(t) = 0$, the relationship $a = b(A_{\max}/A_0 - 1)$ should be held between the model parameters [27].

Recently, Lan *et al.* [30]–[32] developed and validated clinically a 3-D finite-element upper arm model to study the effect of arm soft tissue, muscle, brachial artery, and humerus mechanical properties on oscillometric measurements. They showed that the pressure transmission from the external surface of the arm to the tissue surrounding the brachial artery varies at different longitudinal locations even if the external pressure is uniformly applied along the arm. They defined a pressure transmission ratio as the pressure at the external brachial artery surface divided by the pressure on the arm surface and found that this ratio degrades by up to 70% from the center to the edge of the cuff. This means that the ALA increases from center to the edge of the cuff, and when the artery is closed at the center, it can remain open underneath the rest of the cuff. Since the measured CP in oscillometry is a reflection of the entire arterial area change under the cuff rather than one section, (4) should be modified, accordingly. This is done by adding a small constant A_{cst} to (4), as follows:

$$A_c(t) = A(t) + A_{\text{cst}} = \begin{cases} A_{\text{cst}} + A_0 e^{ap_t(t)}, & \text{for } p_t(t) \leq 0 \\ (A_{\text{cst}} + A_{\max}) + (A_0 - A_{\max})e^{-bp_t(t)}, & \text{for } p_t(t) \geq 0 \end{cases} \quad (5)$$

where $A_c(t)$ represents the average ALA under the oscillometric cuff. The ALA model in (5) is different from (4) only in the constant A_{cst} that represents the average nonzero ALA over the whole cuff bladder width when the arterial area at the center of the cuff is zero. Fig. 1(c) shows the simulated ALA as a function of CP. The following values were used as the average model parameters along the corresponding arterial segment: $a = 0.09$ mmHg⁻¹, $b = 0.03$ mmHg⁻¹, $A_0 = 0.1$ cm², and $A_{\max} = 0.4$ cm² [26]. The constant A_{cst} was set to 5% of the maximum ALA during the deflation which was 0.018 cm². The necessity of the constant A_{cst} in the ALA model will be verified in Section III on estimated PTTs from actual recordings. Nevertheless, we will show in Section II-B that our proposed BP estimation method is independent of the ALA parameters including the constant A_{cst} .

The ALA is composed of two main components: the slow-varying component due to the deflating CP (represented as $\bar{A}_c(t)$ hereafter) and the oscillations due to the arterial pressure (represented as $\tilde{A}_c(t)$ hereafter). Assuming that the arm tissue is mostly incompressible, any change in the arterial volume results in a corresponding change in the cuff bladder volume and as a consequence in the recorded CP [32]. These mechanics can be expressed mathematically using a linear system of equations, as shown in [10]. Over the duration of the cuff deflation, the CP oscillations form a signal known as the oscillometric waveform (OMW) that is proportional to the oscillations of the ALA [10]:

$$\text{OMW}(t) \propto \tilde{A}_c(t). \quad (6)$$

In [10] and [21], the oscillations of the simulated ALA were extracted using a high-pass filter with cutoff frequency of 0.3 Hz [10] to 0.5 Hz [21]. The extracted ALA oscillations were then analyzed and compared with the OMW extracted from the actual recorded CP. It was found that the two waveforms match very closely. However, no mathematical model was proposed for the OMW.

OMW is usually the only signal obtained in oscillometry, and therefore, it is the focus of all oscillometric algorithms to find the BP values [33]. Hence, it is of great importance to obtain a model of the OMW to study, develop, and test the oscillometric algorithms. In this paper, we adopt the same approach we recently proposed in [34] to obtain the OMW model. The slow-varying component of the ALA $\bar{A}_c(t)$ is modeled and subtracted from the whole ALA $A_c(t)$ to obtain a model of the ALA oscillations. The ALA oscillations are due to the periodic nature of arterial pressure, and the slow-varying component of the ALA is due to the deflating CP. Therefore, the slow-varying component can be obtained by fixing the arterial pressure $p_a(t)$

in (5) to its mean MAP, as follows:

$$\bar{A}_c(t) = \begin{cases} A_{cst} + A_0 e^{a(\text{MAP} - p_c(t))}, & \text{for } (\text{MAP} - p_c(t)) \leq 0 \\ (A_{cst} + A_{\max}) + (A_0 - A_{\max}) e^{-b(\text{MAP} - p_c(t))}, & \text{for } (\text{MAP} - p_c(t)) \geq 0 \end{cases} \quad (7)$$

where $p_c(t)$ is the CP. The slow-varying component of the ALA is shown by a dashed line in Fig. 1(c).

According to (6), the OMW model can be obtained as follows:

$$\text{OMW}(t) = \eta (A_c(t) - \bar{A}_c(t)) \quad (8)$$

where η is a scaling factor. Fig. 1(d) shows the simulated OMW using (8) with $\eta = 10 \text{ mmHg/cm}^2$. The peaks, troughs, and zeros of the oscillometric pulses have been marked by upward triangles, downward triangles, and squares, respectively. According to (5), the slope of the ALA monotonically increases as the transmural pressure increases from $-\infty$ to 0, and then it starts to decrease as the transmural pressure increases further from 0 to ∞ . Therefore, at higher CPs and lower arterial pressures, where the transmural pressure becomes more negative and the slope of the ALA is close to zero, the ALA exhibits the lowest amplitude oscillations. As a result, the zero crossing points and the troughs of the oscillometric pulses become very close at high CPs, as is observed in Fig. 1(d). Since parameter a is greater than b , this effect is less visible for zero-crossings and peaks of the oscillometric pulses at low CPs.

As mentioned earlier, the CP deflation rate is usually between 1 and 4 mmHg/s. On the other hand, the arterial pressure changes from DBP to SBP within a heartbeat which has a duration of about 0.6–1.2 s in healthy adults during rest [35]. Therefore, variations of CP are much less than the variations of the arterial pressure in each heartbeat [e.g., see Fig. 1(a)]. As a result, CP $p_c(t)$ and the slow-varying component of the ALA $\bar{A}_c(t)$ can be assumed constant within each heartbeat. Based on the above discussion and according to (5), (7), and (8), it can be concluded that the peaks of the OMW occur when arterial pressure is maximum, i.e. when $p_a(t) = \text{SBP}$. The troughs of the OMW occur when the arterial pressure is minimum, i.e., when $p_a(t) = \text{DBP}$. Also, the OMW crosses zero when the arterial pressure is equal to MAP, i.e., $p_a(t) = \text{MAP}$. This equivalence between the time points at which the arterial pressure is equal to SBP, DBP, and MAP, and the time points at which the OMW is maximum, minimum, and zero, respectively, can be observed in Fig. 1(a) and (d).

The OMW envelope (OMWE) is defined as the amplitude difference between the peaks and troughs of the OMW [10]. Fig. 1(e) shows the OMWE. As was expected [10], [17]–[21], it is obvious that the OMWE has a maximum close to the point at which the CP is equal to MAP. In the conventional oscillometric method, empirical ratios are used to find the time points at which the CP coincides with the SBP and DBP [33]. It has been observed that these ratios should be changed as the parameters of the cardiovascular system vary between different health conditions, age groups, etc. [10], [11]. In the next section, we develop a novel method of estimating SBP, DBP, and MAP that is independent of any parameters.

B. PTT Model

In this section, we prove analytically how the PTT measured at certain points of the arterial pulses can be employed to estimate the SBP, DBP, and MAP. These theoretical findings will be then validated in Section III on real oscillometric measurements.

In oscillometry, cuff affects the propagation of BP pulse wave locally in the brachial artery under the cuff, while the propagation of the BP pulse wave from the heart to the brachial artery is not affected. Therefore, PTT is modeled with two components: the time it takes for the BP pulse wave to arrive from the heart to the brachial artery under the cuff $\tau_0(t)$ and the time it takes for the BP pulse wave to travel in the brachial artery underneath the cuff $\tau_c(t)$ [16], [29]:

$$\tau(t) = \tau_0(t) + \tau_c(t). \quad (9)$$

As our goal is to analyze the changes in PTT as a function of applied CP, we do not take into account the pre-ejection period (PEP) in our model. Since PEP can be treated as a constant at rest and is not sensitive to CP variations, this is a reasonable assumption [29].

PTT can be computed as the inverse of pulse wave velocity (PWV). PWV is a measure of arterial stiffness and is defined as the speed at which the BP pulse wave travels between two sites of the arterial system. According to the Bramwell and Hill equation [35], the PWV between the heart and the brachial artery $\nu_0(t)$ can be expressed as

$$\nu_0(t) = \sqrt{\frac{A(t)}{\rho} \frac{\partial p_t(t)}{\partial A(t)}} \Big|_{p_c(t)=0} \quad (10)$$

and the PWV in the brachial artery underneath the cuff $\nu_c(t)$ can be written as

$$\nu_c(t) = \sqrt{\frac{A_c(t)}{\rho} \frac{\partial p_t(t)}{\partial A_c(t)}} \quad (11)$$

where $\nu_0(t) = L_0/\tau_0(t)$, $\nu_c(t) = L_c/\tau_c(t)$, and ρ is the blood density. L_0 is the length of the arterial branch from the heart to the arm and L_c is the length of the brachial artery under the cuff bladder (cuff bladder width). By the end of this section, it will be shown that our proposed BP estimation method is independent of ρ , L_0 , and L_c . Notice that to obtain $\nu_0(t)$, the general ALA model in (4) has been considered because there is no cuff over the arterial branch from the heart to the arm.

According to (10) and (11), (9) can be rewritten as follows:

$$\tau(t) = L_0 \sqrt{\frac{\rho}{A(t)} \frac{\partial A(t)}{\partial p_t(t)}} \Big|_{p_c(t)=0} + L_c \sqrt{\frac{\rho}{A_c(t)} \frac{\partial A_c(t)}{\partial p_t(t)}} \quad (12)$$

where the first and second terms on the right side of (12) represent $\tau_0(t)$ and $\tau_c(t)$, respectively. Notice that $\nu_0(t)$ and $\nu_c(t)$ model parameters are assumed to be constant and equal to their average value over the corresponding arterial segment.

The PTT, defined in (12), is a function of four variable terms: $A(t)|_{p_c(t)=0}$, $\partial A(t)/\partial p_t(t)|_{p_c(t)=0}$, $A_c(t)$, and $\partial A_c(t)/\partial p_t(t)$. $A_c(t)$ has been already defined in (5). $A(t)|_{p_c(t)=0}$ is obtained

from (4) as follows:

$$A(t)|_{p_c(t)=0} = A_{\max} + (A_0 - A_{\max})e^{-bp_a(t)}. \quad (13)$$

Since at $p_c(t) = 0$, $p_t(t)$ is always greater than zero, the second term in (4) has been used to derive (13). $\partial A(t)/\partial p_t(t)|_{p_c(t)=0}$ is obtained by taking the derivative of (13) as follows:

$$\frac{\partial A(t)}{\partial p_t(t)} \Big|_{p_c(t)=0} = (A_{\max} - A_0)be^{-bp_a(t)} \quad (14)$$

and, finally, $\partial A_c(t)/\partial p_t(t)$ is obtained by taking the derivative of (5) as follows:

$$\frac{\partial A_c(t)}{\partial p_t(t)} = \begin{cases} aA_0e^{ap_t(t)}, & \text{for } p_t(t) \leq 0 \\ (A_{\max} - A_0)be^{-bp_t(t)}, & \text{for } p_t(t) \geq 0. \end{cases} \quad (15)$$

Now, by substituting (5), (13), (14), and (15) into (12), we obtain

$$\tau(t) = \tau_0(t) + \begin{cases} \tau_{c1}(t), & \text{for } p_t(t) \leq 0 \\ \tau_{c2}(t), & \text{for } p_t(t) \geq 0 \end{cases} \quad (16)$$

where

$$\tau_0(t) = L_0 \sqrt{\rho b \left(\frac{1}{1 - \frac{A_{\max} - A_0}{A_{\max}} e^{-bp_a(t)}} - 1 \right)} \quad (17)$$

$$\tau_{c1}(t) = L_c \sqrt{\rho a \left(1 - \frac{1}{1 + \frac{A_0}{A_{cst}} e^{ap_t(t)}} \right)} \quad (18)$$

$$\tau_{c2}(t) = L_c \sqrt{\rho b \left(\frac{1}{1 - \frac{A_{\max} - A_0}{A_{\max} + A_{cst}} e^{-bp_t(t)}} - 1 \right)}. \quad (19)$$

The second term on the right side of (16) represents $\tau_c(t)$.

Fig. 2(a) shows the simulated PTT during cuff deflation period with $L_0 = 70$ cm, $L_c = 10$ cm, and $\rho = 1060$ kg/m³ [36]. The rest of the parameters were the same as the ones used to simulate Fig. 1. The observed oscillations of the PTT are due to the changes in arterial pressure during each heartbeat. The gradual changes in the amplitude and shape of the PTT oscillations are due to the changes in CP.

From (18) and (19), it is observed that $\tau_{c1}(t)$ and $\tau_{c2}(t)$ are functions of $p_t(t) = p_a(t) - p_c(t)$. Since parameter a is always positive, $\tau_{c1}(t)$ is monotonically increasing as the transmural pressure increases. On the other hand, since parameter b is always positive, $\tau_{c2}(t)$ is monotonically decreasing as the transmural pressure increases. This brings us to the conclusion that $\tau_c(t)$ has a maximum at $p_t(t) = 0$, or in other words, when $p_c(t) = p_a(t)$.

From (17), it can be observed that $\tau_0(t)$ is only a function of the arterial pressure $p_a(t)$. Therefore, $\tau_0(t)$ oscillates during each heartbeat as $p_a(t)$ changes. However, $\tau_0(t)$ would be constant if the arterial pressure $p_a(t)$ in (17) is replaced by a fixed value such as SBP, DBP, and MAP. In other words, $\tau_0(t)|_{p_a(t)=\text{SBP}}$, $\tau_0(t)|_{p_a(t)=\text{DBP}}$, and $\tau_0(t)|_{p_a(t)=\text{MAP}}$ are all constants. It should be noted that the arterial elastic properties may change along the arterial branch from the heart to the arm, and therefore, $\tau_0(t)$ model parameters could change at different locations of the arterial branch. In our PTT model, $\tau_0(t)$

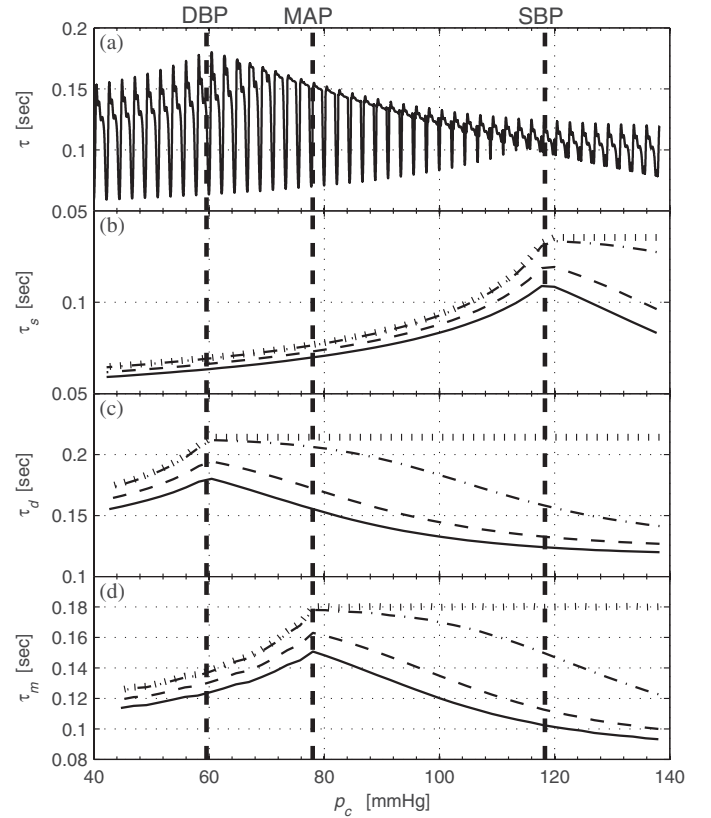


Fig. 2. PTT model. (a) Simulated PTT. (b)–(d) Simulated PTT computed at the points at which the arterial pressure is equal to SBP, DBP, and MAP, respectively. The PTT has been depicted for $A_{cst} = 0\%$, $A_{cst} = 1\%$, $A_{cst} = 10\%$, and $A_{cst} = 20\%$ of the maximum ALA in dotted, dashed-dotted, dashed, and solid lines, respectively.

parameters were assumed to be constant and equal to their average value over the corresponding arterial segment. Also, notice that as we are studying the changes in PTT with respect to the changes in CP applied to the subject's arm, $\tau_0(t)$ is treated as a constant with respect to the CP changes.

If the PTT associated with the points at which arterial pressure equals to SBP, DBP, and MAP, is represented as $\tau_s(t)$, $\tau_d(t)$, and $\tau_m(t)$, respectively, then from the above discussion, it can be concluded that

$$\tau_s(t) \text{ has a maximum at } p_c(t) = \text{SBP} \quad (20)$$

$$\tau_d(t) \text{ has a maximum at } p_c(t) = \text{DBP} \quad (21)$$

$$\tau_m(t) \text{ has a maximum at } p_c(t) = \text{MAP} \quad (22)$$

where

$$\tau_s(t) = \tau(t)|_{p_a(t)=\text{SBP}} \quad (23)$$

$$\tau_d(t) = \tau(t)|_{p_a(t)=\text{DBP}} \quad (24)$$

$$\tau_m(t) = \tau(t)|_{p_a(t)=\text{MAP}}. \quad (25)$$

Therefore, the estimation of the SBP, DBP, and MAP can be performed by finding the CPs at which $\tau_s(t)$, $\tau_d(t)$, and $\tau_m(t)$ have a maximum, respectively, as illustrated in Fig. 2(b)–(d). The same parameter values used in simulation of Fig. 1 were

used in simulation of Fig. 2. The SBP, DBP, and MAP values were determined as the maximum, minimum, and arithmetic mean of the arterial pressure in a cardiac cycle, respectively. The important point is that $\tau_s(t)$, $\tau_d(t)$, and $\tau_m(t)$ always exhibit a maximum independent of the model parameter values at CP equal to SBP, DBP, and MAP, respectively. The only exception is when the constant A_{cst} is equal to zero. In this case, $\tau_s(t)$, $\tau_d(t)$, and $\tau_m(t)$ will exhibit a flat maximum starting at the point at which the CP equals to SBP, DBP, and MAP, respectively. In such a case, the BP values can be determined as the CP at which the slope of PTT becomes zero. However, as explained in Section II-A, the constant A_{cst} is always greater than zero since the arterial branch under the cuff is never occluded completely at typical CP values. The nonzero value of the constant A_{cst} was verified on the PTT curves obtained on real measurements, as will be shown in Section III. $\tau_s(t)$, $\tau_d(t)$, and $\tau_m(t)$ are plotted for $A_{cst} = 0\%$, $A_{cst} = 1\%$, $A_{cst} = 10\%$, and $A_{cst} = 20\%$ of the maximum ALA in Fig. 2(b)–(d), respectively. It should be pointed out that the PEP could alter Fig. 2(a)–(d) by shifting it upward by a small constant. However, PEP does not alter the shape of the PTT curves and location of their maxima as it can be assumed to be constant at rest during the measurement interval [29]. Therefore, our proposed method is independent of the PEP.

C. Experimental Determination of PTT

In this section, we demonstrate how to experimentally measure the PTT from the simultaneous ECG and oscillometric recordings and how the experimental measured PTT is related to the theory developed in the previous section.

In our research, the InBeam prototype [16] was used to record the simultaneous oscillometric BP and ECG signals. PTT was estimated as the time interval between the ECG R-peaks and certain points of the oscillometric pulses, i.e., the peaks, troughs, and zeros.

For the purpose of better illustration, this process is shown on a simulated pulse in Fig. 3. The corresponding arterial pressures at the aorta and the brachial artery are shown in Fig. 3(a) by dashed and solid lines, respectively. The aortic pressure waveform is obtained as the time-shifted version of the brachial artery pressure waveform defined in (3). The amount of time shift was determined according to (16)–(19). The time interval between the ECG R-peak (shown by the bold vertical dashed line) and the aortic pulse peak was set to 30 ms. These values were arbitrarily chosen for the purpose of illustration only. The theoretical PTTs associated with the points at which the arterial pressure equals SBP, DBP, and MAP are shown in Fig. 3(a) as τ_s , τ_d , and τ_m , respectively. In theory, these PTTs can be computed through (23)–(25), respectively. However, in experiment, the PTT is estimated as the time interval between the ECG R-peaks and the oscillometric peaks, troughs, and zeros, as shown Fig. 3(b). The estimated PTTs are shown as τ_p , τ_t , and τ_z , respectively. As it can be observed from Fig. 3, there is a time difference between the estimated and the theoretical PTTs that have been shown as T_s , T_d , and T_m . T_s , T_d , and T_m are the time intervals between the ECG R-peak and the time points at which the aortic pulse

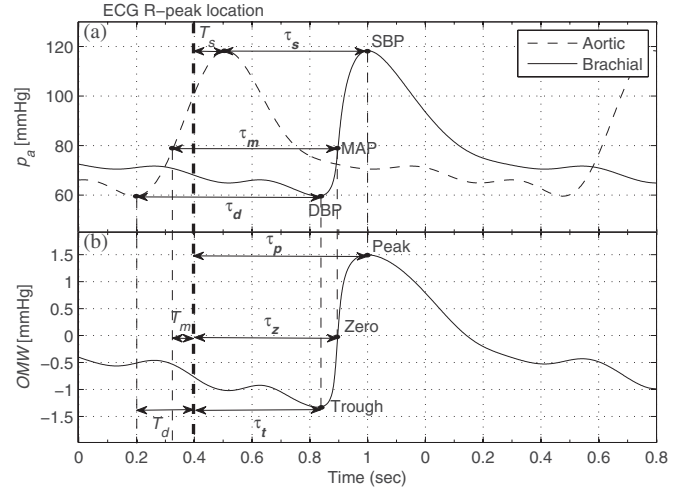


Fig. 3. Experimental determination of PTT shown on simulated pulses for a better illustration. (a) Simulated arterial pressure waveforms in the aorta and the brachial artery. (b) Simulated OMW. $\tau_s(t)$, $\tau_d(t)$, and $\tau_m(t)$ represent the theoretical PTTs that can be computed through (23)–(25), respectively. $\tau_p(t)$, $\tau_t(t)$, and $\tau_z(t)$ are the experimentally measured PTTs according to (29)–(31), respectively. The bold vertical dashed line shows the ECG R-peak location in both figures.

is equal to SBP, DBP, and MAP, respectively. It is obvious that these time intervals are independent of the CP that is applied to the brachial artery. Therefore, they are assumed to be constant during the deflation period. As a result, (20)–(22) can be rewritten for $\tau_p(t)$, $\tau_t(t)$, and $\tau_z(t)$, as follows:

$$\tau_p(t) \text{ has a maximum at } p_c(t) = \text{SBP} \quad (26)$$

$$\tau_t(t) \text{ has a maximum at } p_c(t) = \text{DBP} \quad (27)$$

$$\tau_z(t) \text{ has a maximum at } p_c(t) = \text{MAP} \quad (28)$$

where

$$\tau_p(t) = \tau_s(t) + T_s \quad (29)$$

$$\tau_t(t) = \tau_d(t) - T_d \quad (30)$$

$$\tau_z(t) = \tau_m(t) - T_m. \quad (31)$$

Equations (26)–(28) provide the means to estimate SBP, DBP, and MAP, respectively, independent of any parameters.

III. EXPERIMENTAL RESULTS

A. Pilot Study

As an initial validation of our proposed method, we tested it on real-world data. This dataset comprised 150 simultaneous oscillometric BP and ECG recordings (acquired with the InBeam prototype [16]) from ten healthy subjects—six males and four females—aged from 24 to 63 years. This study was approved by the University of Ottawa Research Ethics Board and written informed consent was obtained from all subjects. To the best of our knowledge, no subject had a history of cardiovascular or respiratory disease. Recordings from each subject were obtained on three separate days with five sets of recordings on each day.

Each set of recordings started with the Omron measurement on the right arm. As soon as the Omron measurement ended,

the InBeam prototype measurement started on the left arm. The subject also wore the wristband of the InBeam prototype on the right wrist for simultaneous ECG recording. Since the American Heart Association recommends at least a 1-min gap between two consecutive BP measurements [1], the five sets of measurements were performed with 3-min gaps. Although there may be differences in BP measured from right and left arms, studies have shown that such differences are not statistically significant in healthy subjects [37] such as the ones tested in this pilot investigation.

The InBeam recordings comprised inflating the prototype cuff to a pressure of 160 mmHg and then deflating it slowly to a pressure of 20 mmHg. The deflation rate was 1.5–3.5 mmHg/s. Following the measurement, the InBeam oscillometric and ECG signals corresponding to a CP range of 25–155 mmHg were chosen for further analysis. The ranges of the reference recorded SBPs and DBPs were 79–136 and 52–86 mmHg, respectively. Since the Omron device only provides the SBP and DBP values, the reference MAP was calculated using the common formula $MAP = DBP + 1/3 \times (SBP - DBP)$ [35], for all comparisons and analysis.

B. OMW Detection

As explained in Section II-C, our proposed BP estimation method is based on measuring the time interval between the ECG R-peaks and the peaks, troughs, and zeros of the OMW. Therefore, detection of the correct location of peaks, troughs, and zeros of the OMW is of great importance.

1) *Detecting the Peaks and Troughs*: In order to find the peaks and troughs of the OMW, an ECG-based detrending approach was utilized [16]. The R-peaks of the ECG signal were first found using the MIT/PhysioNET MATLAB QRS onset detector software [38]. Fig. 4(a) shows a sample ECG signal from the database with the detected R-peaks marked in dots. The CP values corresponding to the detected R-peaks were then interpolated to form a detrended CP signal. Fig. 4(b) illustrates the recorded CP in solid black line. The detrended CP signal using the explained ECG-based technique is plotted in dashed light gray line (visible in inset). The OMW was found by subtracting the detrended from the original CP signal, as shown in Fig. 4(c). The peaks and troughs of the OMW were detected with the help of ECG R-peaks. The oscillometric peaks and troughs were determined as the maximum and the minimum of the extracted OMW between each two consecutive R-peaks, respectively. The detected peaks and troughs of the OMW are shown with upward and downward triangles in Fig. 4(c). Despite high-pass filtering techniques [10], [21] that can alter the peaks and troughs locations depending on the filter parameters, the utilized ECG-based method can find the exact location of the OMW peaks and troughs without any approximation.

2) *Detecting the Zero-Crossings*: Although the ECG-based OMW detection method is very accurate in determining the location of the peaks and troughs, it cannot completely remove the slow-varying component of the CP, and therefore, it introduces some bias to the oscillometric pulses. This makes it challenging to find the correct location of the OMW zero-crossings.

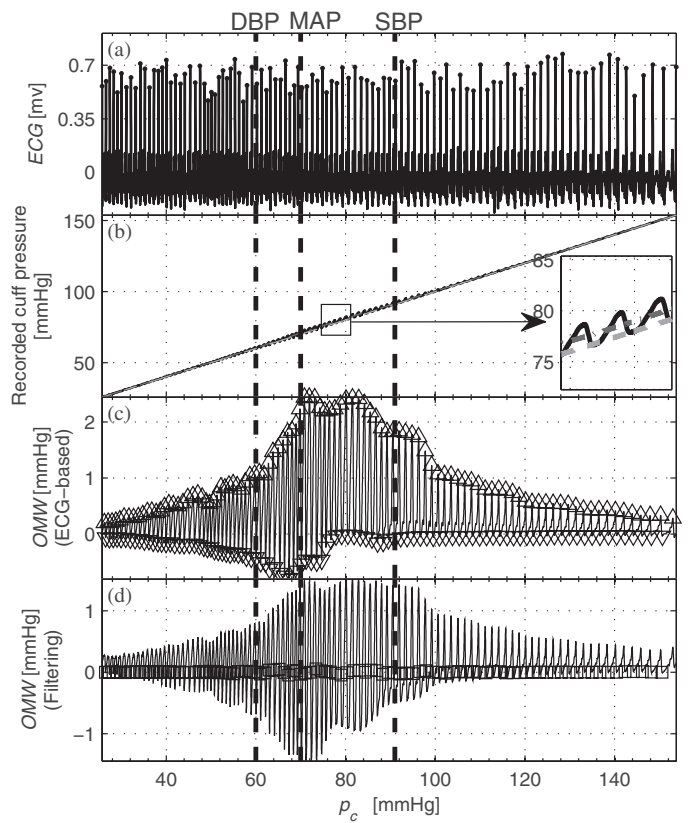


Fig. 4. OMW detection. (a) Real ECG signal. (b) Recorded CP [simultaneous with the ECG shown in (a)]. The detrended CPs using the ECG-based method and the filtering technique are depicted in dashed and dashed-dotted lines in the same figure, respectively, which can be seen more clearly in the inset. (c) OMW obtained using the ECG-based method. The peaks and troughs are shown in upward and downward triangles, respectively. (d) OMW obtained through filtering. The zeros of the OMW are shown in squares.

Therefore, in order to detect the zeros of the OMW, we adopt a filtering approach. In this method, we find the detrended CP waveform by applying a low-pass filter on the recorded CP. The detrended CP signal is then subtracted from the original CP signal to form the OMW. The detrended CP signal is plotted in dashed-dotted dark gray line in Fig. 4(b) and is visible in the inset. Fig. 4(d) depicts the OMW obtained by subtracting the detrended signal from the original CP signal. The zeros are marked in squares in the figure.

3) *Forming the OMWE*: In order to find the OMWE, the consecutive peaks and troughs of the OMW (detected using the ECG-based approach) were subtracted and plotted against the CP, as shown by the gray line in Fig. 5(a). The OMWE was smoothed using a seven-point moving average filter. A cubic smoothing spline function with smoothing parameter 0.1 was then fitted to the smoothed signal. The resulted signal is shown by the black line in Fig. 5(a). As it can be observed, the peak of the OMWE is very close to the reference MAP as it was expected from the theoretical model.

C. PTT Detection

$\tau_p(t)$, $\tau_t(t)$, and $\tau_z(t)$ were measured as the time interval between the ECG R-peaks and the peaks, troughs, and zeros of

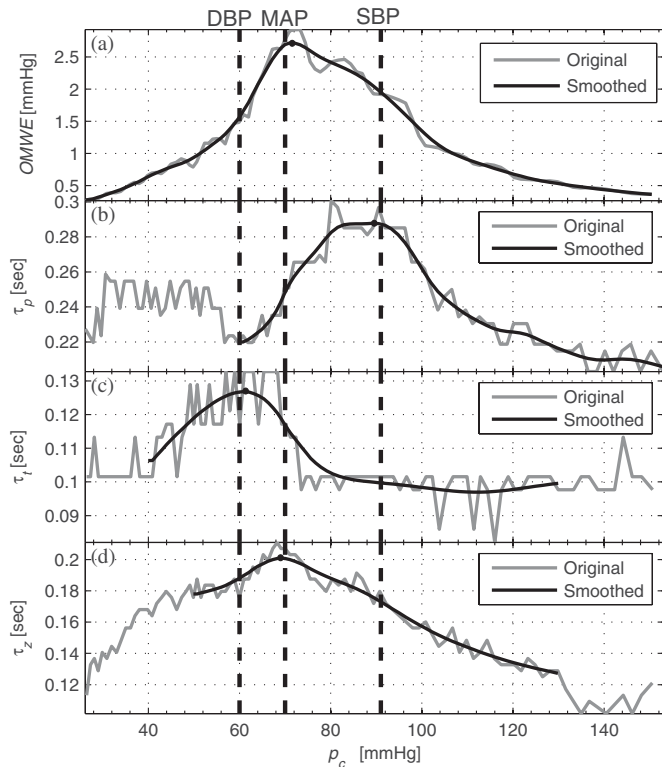


Fig. 5. Detected OMWE and PTT. (a) OMWE. (b)–(d) PTT computed as the time interval between the ECG R-peaks and the peaks, troughs, and zeros of the OMW, respectively.

the OMW, respectively. The calculated $\tau_p(t)$, $\tau_t(t)$, and $\tau_z(t)$ are plotted in the gray lines in Fig. 5(b)–(d), respectively. Since the calculated PTTs are very noisy, several steps are performed before determining their true maximum, as follows:

1) *Outlier Removal*: An outlier removal technique was applied to remove the PTT samples that appear to be inconsistent with the remainder of the signal. The adopted outlier removal technique in this paper was based on fitting a quadratic polynomial function to the PTT waveforms. An outlier was defined as a value that is more than three standard deviations away from the quadratic polynomial fit [39]. The outliers were then removed and this procedure was repeated until no more outliers were detected.

2) *Smoothing*: The PTTs were first smoothed using a moving average filter. Afterward, a cubic smoothing spline function was fitted to the smoothed signal to remove any remaining artifacts. Since $\tau_t(t)$ exhibited the most fluctuations, a nine-point moving average filter and a spline function with smoothing parameter 0.01 were used to smooth the signal. On the other hand, $\tau_p(t)$ exhibited the least fluctuations around its peak, and therefore, it was smoothed using a three-point moving average filter and a spline function with smoothing parameter 0.2. $\tau_z(t)$ was smoothed using a seven-point moving average filter and a spline function with smoothing parameter 0.02. The filter parameters used in this study were chosen empirically.

3) *Maximum Detection*: The smoothed PTTs were linearly interpolated and resampled at 5 Hz. In order to avoid any remaining noise and artifacts, the search region for maximum

TABLE I
ME, SDE, AND MAE OF THE COEFFICIENT-FREE BP ESTIMATES

	PTT-based			OMWE-based
	SBP	DBP	MAP	MAP
ME [mmHg]	3.09	2.39	5.31	1.25
SDE [mmHg]	5.81	5.78	4.30	7.32
MAE [mmHg]	5.31	4.51	5.74	4.63

was limited. For detection of $\tau_z(t)$ maximum, the search was performed from $p_c(t) = 55$ mmHg to $p_c(t) = 140$ mmHg. For detection of $\tau_p(t)$ maximum, the search was performed from $p_c(t) = (\text{MAP} + 12)$ mmHg to $p_c(t) = 150$ mmHg. For detection of $\tau_t(t)$ maximum, the search was performed from $p_c(t) = 50$ mmHg to $p_c(t) = (\text{MAP} - 5)$ mmHg. MAP was estimated as the CP at which $\tau_z(t)$ has a maximum. These limits were preliminary choices based on the available data.

The resulting $\tau_p(t)$, $\tau_t(t)$, and $\tau_z(t)$ after outlier removal and smoothing are depicted in solid black lines in Fig. 5(b)–(d), respectively. The smoothed PTTs are only plotted in the limited interval where the search for the maximum is performed. Note that the PTTs depicted in Fig. 5(b)–(d) are consistent with those computed theoretically [shown in Fig. 2(b)–(d)].

D. Results on the Whole Dataset

The performance of our proposed BP estimation algorithm was tested on the whole recorded dataset introduced in Section III-A. The estimation results were compared with the FDA-approved Omron oscillometric BP monitor (HEM-790IT) as the reference. The performance was analyzed in terms of mean error (ME), standard deviation of error (SDE), and MAE. ME is a measure of the bias of BP estimates. SDE is a measure of error variability. A method with small ME can still be unreliable if it produces large values of SDE. MAE is a measure of the overall accuracy in estimating the BP. Smaller values of MAE correspond to better overall performance.

Table I summarizes the values of ME, SDE, and MAE for our proposed coefficient-free BP estimation method obtained on the dataset of 150 recordings. The coefficient-free MAP estimation errors based on the OMWE are also reported in the last column of the table. It is observed that the ME of our proposed method in estimating systolic and diastolic pressures is within 3.09 mmHg of the Omron device, the SDE of our proposed method in estimating systolic and diastolic pressures is within 5.81 mmHg of the Omron device, and the MAE of our proposed method in estimating systolic and diastolic pressures is within 5.31 mmHg of the Omron device. Comparing the PTT-based and the OMWE-based methods, it is observed that the PTT-based method achieves smaller SDE, while the conventional OMWE-based method achieves smaller values in ME and MAE.

In order to further analyze the agreement between our proposed method and the Omron monitor, we performed the Bland–Altman analysis. Fig. 6 shows the Bland–Altman plot of the SBP, DBP, and MAP estimates for our proposed method versus Omron monitor. The x -axis of the plots shows the average of our proposed method and the Omron monitor, while the y -axis

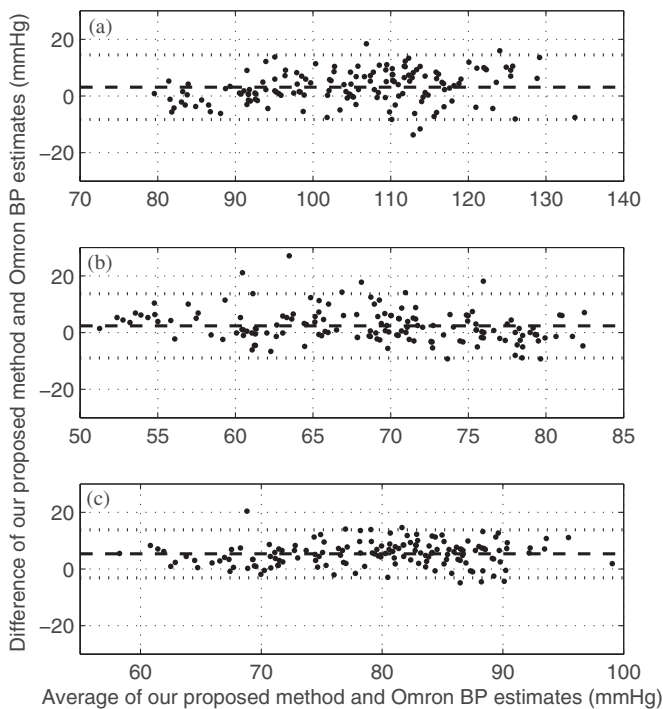


Fig. 6. Bland–Altman plot of the (a) systolic, (b) diastolic, and (c) mean blood pressure estimates for our proposed method versus Omron monitor. The horizontal dotted lines show the limits of agreement, while the horizontal dashed line shows the bias.

shows the difference between the two devices. The bias (ME) and the limits of agreement ($\text{bias} \pm 1.96 \times \text{standard deviation or error}$) are shown in dashed and dotted lines, respectively. It is observed that, for all the plots, the majority of the points lie within the limits of agreement. That is, the BP estimates made by our proposed method are in close agreement with those made by the Omron device. The biases for SBP, DBP, and MAP estimates are 3.09, 2.39, and 5.31 mmHg, respectively.

IV. CONCLUSION

We presented a comprehensive theory and developed a model for the dependence of PTT on CP within an oscillometric BP measurement framework. Through this model, we analytically showed that SBP, DBP, and MAP can be accurately estimated from PTT–CP mappings without using empirical coefficients. Finally, we cross-validated our findings on 150 recordings (oscillometric and ECG) from ten healthy subjects and compared results with the FDA-approved Omron monitor. The theoretical model and the empirical results conformed well to the reference measurements. For comparison with the Omron device, the method achieved an MAE of 5.31 mmHg for SBP, 4.51 mmHg for DBP, and 5.74 mmHg for MAP.

This is the first study in which a mathematical validation was provided for the theory of BP estimation from PTT–CP dependence. Moreover, it is the first study to propose a nonparametric PTT-based BP estimation method within an oscillometric measurement framework. The theoretical model for the PTT–CP

analysis was developed from earlier works which focused solely on oscillometric BP measurement models.

V. LIMITATIONS AND FUTURE WORK

Possible limitations of this study are as follows: 1) we validated our proposed method against the Omron HEM-790IT BP monitor as the reference, while the ideal references could have been either based on the noninvasive auscultatory or the invasive intra-arterial methods; 2) the method was tested on a modest cohort of ten healthy subjects and no patients were investigated; and 3) we assumed that the various parameters inside our model do not change with cuff deflation during a measurement.

However, it should be noted that the FDA-approved Omron HEM-790IT has gone through rigorous clinical validation according to protocols set forth by the European Society of Hypertension, Association for the Advancement of Medical Instruments, and BHS [40]–[42]. Therefore, for this pilot study, the successful validation of our proposed method against the Omron monitor is sufficient to support its potential significance and efficacy.

It should be also pointed out that although the number of subjects was 10, to increase the statistical significance of the empirical data, we recorded 15 simultaneous ECG and oscillometric BP signals from every participant (five recordings in three days). This resulted in a substantial dataset of 150 recordings for the pilot investigation. Future work will involve undertaking clinical testing on a larger number of healthy subjects as well as patients, whereby the method will be compared against nurse-recorded auscultatory measurements, and if possible, against invasive measurements.

We also understand that for certain patient populations and disease states, such as atrial fibrillation, the PTT model parameters may well change during a measurement which may be as short as 30–45 s. Therefore, future work will focus on models that incorporate the time variability of these parameters.

ACKNOWLEDGMENT

The authors declare that they have founded a company called Health Parametrics Inc. to commercialize the ECG-assisted BP monitoring technology. They have also submitted patent applications in the U.S., U.K., and Canada, with regard to this technology.

REFERENCES

- [1] T. G. Pickering, J. E. Hall, L. J. Appel, B. E. Falkner, J. Graves, M. N. Hill, D. W. Jones, T. Kurtz, S. G. Sheps, and E. J. Roccella, “Recommendations for blood pressure measurement in humans and experimental animals—part 1: Blood pressure measurement in humans: A statement for professionals from the subcommittee of professional and public education of the American Heart Association Council on high blood pressure research,” *Hypertension*, vol. 45, pp. 142–161, Dec. 2005.
- [2] K. R. Dobbin, “Noninvasive blood pressure monitoring,” *Crit. Care Nurse*, vol. 22, pp. 123–124, Apr. 2002.
- [3] J. Handler, “The importance of accurate blood pressure measurement,” *Perm. J.*, vol. 13, pp. 51–54, 2009.
- [4] P. D. Baker, D. R. Westenskow, and K. Kuck, “Theoretical analysis of non-invasive oscillometric maximum amplitude algorithm for estimating mean blood pressure,” *Med. Biol. Eng. Comput.*, vol. 35, pp. 271–278, 1997.

- [5] Z. M. Anastas, E. Jimerson, and S. Garolis, "Comparison of noninvasive blood pressure measurements in patients with atrial fibrillation," *J. Cardiovasc. Nurs.*, vol. 23, pp. 519–524, 2008.
- [6] M. T. Guagnano, V. P. Palitti, R. Murri, L. Marchione, D. Merlitti, and S. Sensi, "Many factors can affect the prevalence of hypertension in obese patients: Role of cuff size and type of obesity," *Panminerva Med.*, vol. 40, pp. 22–27, 1998.
- [7] G. Beevers, G. Y. H. Lip, and E. O'Brien, "Abc of hypertension: Blood pressure measurement: Part I-sphygmomanometry: Factors common to all techniques," *Brit. Med. J.*, vol. 322, pp. 981–985, 2001.
- [8] C. Sala, E. Santin, M. Rescaldani, C. Cuspidi, and F. Magrini, "What is the accuracy of clinic blood pressure measurement?," *Amer. J. Hypertens.*, vol. 18, pp. 244–248, 2005.
- [9] C. A. Lodi, C. Estridge, and C. Ghidini, "In vitro and in vivo evaluation of an oscillometric device for monitoring blood pressure in dialysis patients," *Nephrol. Dial. Transplant.*, vol. 22, pp. 2950–2961, 2007.
- [10] G. Drzewiecki, R. Hood, and H. Apple, "Theory of the oscillometric maximum of the systolic and diastolic detection ratios," *Ann. Biomed. Eng.*, vol. 22, pp. 88–96, Jan. 1994.
- [11] J. Talts, R. Raamat, K. Jagomagi, and J. Kivastik, "An influence of multiple affecting factors on characteristic ratios of oscillometric blood pressure measurement," in *Proc. 15th Nordic-Baltic Conf. Biomed. Eng. Med. Phys.*, Aalborg, Denmark, Jun. 2011, pp. 73–76.
- [12] L. A. Geddes, M. Voelz, S. James, and D. Reiner, "Pulse arrival time as a method of obtaining systolic and diastolic blood pressure indirectly," *Med. Biol. Eng. Comput.*, vol. 19, pp. 671–672, 1981.
- [13] T. Sharir, A. Marmor, C.-T. Ting, J.-W. Chen, C.-P. Liu, M.-S. Chang, F. C. P. Yin, and D. A. Kass, "Validation of a method for noninvasive measurement of central arterial pressure," *Hypertension*, vol. 21, pp. 74–82, 1993.
- [14] J. Kerola, V. Kontra, and R. Sepponen, "Non-invasive blood pressure data acquisition employing pulse transit time detection," in *Proc. 18th Annu. Int. Conf. IEEE Eng. Med. Biol. Soc.*, Amsterdam, Netherlands, Oct./Nov. 1996, pp. 1308–1309.
- [15] H. Sorvoja, R. Myllylä, P. Kärjä-Koskenkari, J. Koskenkari, M. Lilja, and Y. Antero, "Accuracy comparison of oscillometric and electronic palpation blood pressure measuring methods using intra-arterial method as a reference," *Mol. Quant. Acoust.*, vol. 26, pp. 235–260, 2005.
- [16] S. Ahmad, S. Chen, K. Soueidan, I. Batkin, M. Bolic, H. Dajani, and V. Groza, "Electrocardiogram-assisted blood pressure estimation," *IEEE Trans. Biomed. Eng.*, vol. 59, no. 3, pp. 608–618, Mar. 2012.
- [17] G. Drzewiecki, "Noninvasive assessment of arterial blood pressure and mechanics," in *The Biomedical Engineering Handbook*, J. D. Bronzino, Ed. Boca Raton, FL: CRC Press, 1999, pp. 2367–2374.
- [18] G. W. Mauck, C. R. Smith, L. A. Geddes, and J. D. Bourland, "The meaning of the point of maximum oscillations in cuff pressure in the indirect measurement of blood pressure—part ii," *J. Biomech. Eng.*, vol. 102, no. 1, pp. 28–33, 1980.
- [19] F. K. Forster and D. Turney, "Oscillometric determination of diastolic, mean, and systolic blood pressure. A numerical model," *ASME J. Biomech. Eng.*, vol. 108, pp. 359–364, Nov. 1986.
- [20] W. T. Link, "Techniques for obtaining information associated with an individual's blood pressure including specifically a stat mode technique," U.S. Patent 4 664 126, Oct. 13, 1987.
- [21] M. Ursino and C. Cristalli, "A mathematical study of some biomechanical factors affecting the oscillometric blood pressure measurement," *IEEE Trans. Biomed. Eng.*, vol. 43, no. 8, pp. 761–778, Aug. 1996.
- [22] B. Balasingam, M. Forouzanfar, M. Bolic, H. R. Dajani, V. Z. Groza, and S. Rajan, "Arterial blood pressure parameter estimation and tracking using particle filters," in *Proc. IEEE Int. Workshop Med. Meas. Appl.*, Bari, Italy, May 2011, pp. 473–476.
- [23] M. Saeed, M. Villarroel, A. T. Reisner, G. Clifford, L.-W. Lehman, G. Moody, T. Heldt, T. H. Kyaw, B. Moody, and R. G. Mark, "Multi-parameter intelligent monitoring in intensive care ii (mimic-ii): A public-access intensive care unit database," *Crit. Care Med.*, vol. 39, pp. 952–960, May 2011.
- [24] D. J. Hughes, C. F. Babbs, L. A. Geddes, and J. D. Bourland, "Measurements of young's modulus of elasticity of the canine aorta with ultrasound," *Ultrason. Imag.*, vol. 1, pp. 356–367, 1979.
- [25] H. H. Hardy and R. E. Collins, "On the pressure-volume relationship in circulatory elements," *Med. Biol. Eng. Comput.*, vol. 20, pp. 565–570, 1982.
- [26] S. Sun, "A total compliance method for noninvasive arterial blood pressure measurement," Ph.D. dissertation, School Med., Univ. Utah, Salt Lake City, USA, 1990.
- [27] J. S. Clark and S. Sun, "Total compliance method and apparatus for noninvasive arterial blood pressure measurement," U.S. Patent 5 423 322, Jun. 13, 1995.
- [28] R. Raamat, J. Talts, K. Jagomagi, and E. Länsimies, "Mathematical modelling of non-invasive oscillometric finger mean blood pressure measurement by maximum oscillation criterion," *Med. Biol. Eng. Comput.*, vol. 37, no. 6, pp. 784–788, Nov. 1999.
- [29] X. F. Teng and Y. T. Zhang, "Theoretical study on the effect of sensor contact force on pulse transit time," *IEEE Trans. Biomed. Eng.*, vol. 54, no. 8, pp. 1490–1498, Aug. 2007.
- [30] H. Lan, A. M. Al-Jumaily, and A. Lowe, "An investigation into the upper arm deformation under inflatable cuff," in *Proc. Int. Mech. Eng. Congr. Expo.*, Boston, MA, USA, Oct. 2008, pp. 1–4.
- [31] H. Lan, A. M. Al-Jumaily, W. Hing, and A. Lowe, "Biomechanical basis of oscillometric blood pressure measuring technique," in *Proc. Int. Mech. Eng. Congr. Expo.*, Lake Buena Vista, FL, USA, Nov. 2009, pp. 1–4.
- [32] H. Lan, A. M. Al-Jumaily, A. Lowe, and W. Hing, "Effect of tissue mechanical properties on cuff-based blood pressure measurements," *Med. Eng. Phys.*, vol. 33, no. 10, pp. 1287–1292, Dec. 2011.
- [33] S. Chen, V. Z. Groza, M. Bolic, and H. R. Dajani, "Assessment of algorithms for oscillometric blood pressure measurement," in *Proc. IEEE Int. Instrum. Meas. Technol. Conf.*, Singapore, May 2009, pp. 1763–1767.
- [34] M. Forouzanfar, B. Balasingam, H. R. Dajani, V. Groza, M. Bolic, S. Rajan, and E. M. Petriu, "Mathematical modeling and parameter estimation of blood pressure oscillometric waveform," in *Proc. IEEE Int. Symp. Med. Meas. Appl.*, Budapest, Hungary, May 2012, pp. 208–213.
- [35] W. W. Nichols and M. F. O'Rourke, *McDonald's Blood Flow in Arteries: Theoretical, Experimental and Clinical Principles*, 4th ed., London, UK: Hodder Arnold Publishers, 1998.
- [36] B. E. Westerhof, I. Guelen, W. J. Stok, K. H. Wesseling, J. A. E. Spaan, N. Westerhof, W. J. Bos, and N. Stergiopoulos, "Arterial pressure transfer characteristics: Effects of travel time," *Amer. J. Physiol. Heart Circ. Physiol.*, vol. 292, pp. H800–H807, Sep. 2007.
- [37] K. Eguchi, M. Yacoub, J. Jhalani, W. Gerin, J. E. Schwartz, and T. G. Pickering, "Consistency of blood pressure differences between the left and right arms," *Arch. Intern. Med.*, vol. 167, pp. 388–393, 2007.
- [38] Harvard-MIT Health Sciences and Technology. (2010, Aug.). QRS Onset Detector. [Online]. Available: <http://www.mit.edu/gari/CODE/ECGtools/ecgBag/sqrs.m>
- [39] D. Ruan, G. Chen, and E. E. Kerre, *Intelligent Data Mining: Techniques And Applications*. New York, USA: Springer, 2005.
- [40] *Automatic Blood Pressure Monitor With ComFit™ Cuff: Model HEM-790IT*, Omron Healthcare Inc., Bannockburn, IL, USA, 2006.
- [41] R. N. Feghali, J. A. Topouchaian, B. M. Pannier, H. A. El Assaad, and R. G. Asmar, "Validation of the omron m7 (hem-780-e) blood pressure measuring device in a population requiring large cuff use according to the international protocol of the European Society of Hypertension," *Blood Press. Monit.*, vol. 12, pp. 173–178, 2007.
- [42] A. Coleman, S. Steel, P. Freeman, A. de Greeff, and A. Shennan, "Validation of the omron m7 (hem-780-e) oscillometric blood pressure monitoring device according to the British Hypertension Society Protocol," *Blood Press. Monit.*, vol. 13, pp. 49–54, 2008.

Mohamad Forouzanfar (S'07) received the B.Sc. degree in electrical engineering from the Ferdowsi University of Mashhad, Mashhad, Iran, in 2004 and the M.Sc. degree (Hons.) in biomedical engineering from the Khajeh Nasir (K.N.) Toosi University of Technology, Tehran, Iran, in 2007. He is currently working toward the Ph.D. degree in electrical and computer engineering at the University of Ottawa, Ottawa, ON, Canada.

From 2005 to 2008, he was a Research Assistant with the Biomedical Imaging Laboratory, K.N. Toosi University of Technology. Since 2009, he has been a Research Assistant with the Biomedical Instrumentation and Processing Research Group, University of Ottawa. His research interests include biomedical signal and image processing, pattern recognition, and neural networks.

Mr. Forouzanfar has served as an organizing committee member in 2010 IEEE International Workshop on Medical Measurement and Applications, and 2010 IEEE Workshop on Adverse Response Monitoring. He is currently on the Student Editorial Board of the IEEE JOURNAL OF TRANSLATIONAL ENGINEERING IN HEALTH AND MEDICINE.

Saif Ahmad received the B.Sc. degree in electrical engineering from Aligarh Muslim University, Aligarh, India, in 1996, the M.Sc. degree in computer science from the University of Birmingham, Birmingham, U.K., in 2001, and the Ph.D. degree in computer science from the University of Surrey, Guildford, U.K., in 2007.

He is currently a Research Associate in the School of Electrical Engineering and Computer Science, University of Ottawa, Ottawa, ON, Canada. Prior to this, he was a Postdoctoral Fellow in the Divisions of Thoracic Surgery and Critical Care Medicine at the Ottawa General Hospital, Canada. He has over three years of industrial experience related to high-voltage engineering, electrical power generation and distribution, and electrical machines at Tata Chemicals Ltd., India. He has published more than 14 papers in peer-reviewed journals and conference proceedings. In 2009, his work on heart rate variability analysis for the diagnosis, prognosis, and prediction of sepsis was published in *PLoS One* and *Critical Care*. This work was also accorded prominent coverage by the Ottawa Citizen. He has served as a reviewer for several IEEE and medical journals as well as conference proceedings. His major research interests include medical device development, biomedical signal processing, and financial time series analysis.

Izmail Batkin received the M.S. and Ph.D. degrees in theoretical physics from the Voronezh State University, Voronezh, Russia, in 1965 and 1969, respectively, and the Dr.Sci. degree in nuclear physics from the Leningrad State University, Saint Petersburg, Russia, in 1982.

He is currently a Research Consultant in the School of Electrical Engineering and Computer Science, University of Ottawa, Ottawa, ON, Canada, and at Ottawa General Hospital, Ottawa. He is also the Chief Scientist at Biopeak Corporation, Ottawa. Prior to this, he was a Professor at the Voronezh State University, and an Adjunct Professor at Carleton University, Ottawa. Over the years, his research has focused on noninvasive monitoring of physiological parameters. He has been involved in the successful development and testing of a new generation of wearable physiological electrodes and monitors for the home and clinical environments. He has obtained one patent and published more than 150 refereed papers many in top notch journals such as *Physical Review*, the *Journal of Physics*, and the *Soviet Journal of Nuclear Physics*. His major research interests include theoretical and nuclear physics, and medical physics.

Hilmi R. Dajani (M'07–SM'11) received the B.Eng. degree in electrical engineering from McMaster University, Hamilton, ON, Canada, in 1987, and the M.Sc. and Ph.D. (collaborative program in biomedical engineering) degrees in electrical and computer engineering from the University of Toronto, Toronto, ON, in 1991 and 2004.

He is currently an Assistant Professor in the School of Electrical Engineering and Computer Science, University of Ottawa. He has several years of experience in implementing technical projects in a hospital setting and in the biomedical technology industry. His research interests include speech-evoked potentials, auditory-inspired speech processing, the development of instrumentation for the assessment and treatment of speech and hearing impairments, and the development of new methods for the analysis of cardiorespiratory function.

Voicu Z. Groza (M'97–SM'02–F'11) received the Dipl.Eng. degree in computer engineering and the Dr.Eng. degree in electrical engineering from the Polytechnic Institute of Timisoara, Timisoara, Romania, in 1972 and 1985, respectively.

He was a Professor with the Polytechnic University of Timisoara. In 1997, he joined the University of Ottawa, Ottawa, ON, Canada, where he is currently with the School of Electrical Engineering and Computer Science, Information Technology and Engineering. He is the author or a coauthor of more than 200 technical papers. His research interests include biomedical instrumentation and measurement, and reconfigurable computers.

Dr. Groza has served as a Conference or Technical Program Chair at several major international events such as the IEEE International Workshop on Medical Measurement and Applications (MeMeA 2008 2013), the 2005 IEEE International Conference on Instrumentation and Measurement, and the 2006 IEEE Canadian Conference on Electrical and Computer Engineering. He is currently the Chair of the IEEE Working Group on Standard for Objective Measurement of Systemic Arterial Blood Pressure in Humans.

Miodrag Bolic (M'04–SM'08) received the B.Sc. and M.Sc. degrees from the University of Belgrade, Belgrade, Serbia, in 1996 and 2001, respectively, and the Ph.D. degree from Stony Brook University, Stony Brook, NY, USA, in 2004, all in electrical engineering.

From 1996 to 2000, he was a Research Associate with the Institute of Nuclear Sciences, Vinča, Belgrade, Serbia. Since 2004, he has been with the University of Ottawa, Ottawa, ON, Canada, where he is Associate Professor in the School of Electrical Engineering and Computer Science. He is a Director of Computer Architecture, RFID, and Medical Devices research groups at the University of Ottawa. He published about 40 journal papers, four book chapters, and edited one book. He has been involved in organization of a number of conferences. His research interests include biomedical signal processing and instrumentation, computer architectures, and wireless communications.